Int. J. Anal. Appl. (2025), 23:147

International Journal of Analysis and Applications

Global Analysis of r3LCMV Cancer Immunotherapy Model

Afnan D. Al Agha*

Department of Mathematical Science, College of Engineering, University of Business and Technology, Jeddah 21361, Saudi Arabia

**Corresponding author:* a.alagha@ubt.edu.sa

Abstract. An attenuated lymphocytic choriomeningitis virus (r3LCMV) has shown safety and efficacy in treating cancer. This paper develops a within-host r3LCMV cancer immunotherapy model. The model considers the interconnection between nutrient, normal cells, tumor cells, infected tumor cells, viral vector, and virus-specific CTLs. The nonnegativity and boundedness of the solutions are verified. The equilibrium points with the biological acceptance conditions are calculated. The global stability of each point is demonstrated. Numerical simulations are implemented to ratify the theoretical results. It is found that the equilibria exhibit four main states: a healthy individual who does not have cancer, a cancer patient who does not receive any treatments, a cancer patient who receives r3LCMV cancer therapy with inactive immunity, and a cancer patient who receives r3LCMV therapy with active virus-specific CTLs. The parameters that control the transition between these states need to be carefully chosen. Increasing the stimulation rate of CTLs induced by r3LCMV viral vector reduces the concentration of infected tumor cells. The attenuation rate of the viral vector affects its ability to eliminate tumor cells from the body. Therefore, these rates need to be cautiously selected and tested.

1. Introduction

Cancer is a major contributor to global deaths. In 2022, approximately 20 million cancer cases were detected, and 9.7 million people died from cancer [1]. The number of cancer cases is expected to reach 35 million by 2050 [1]. Immunosuppression in cancer patients affects the ability of the immune system to eliminate tumor cells [2]. Immunotherapies like immune checkpoint inhibitors have been developed to overcome immunosuppression. However, this type of treatment has been effective in only 30% of patients [2]. Oncolytic virotherapy (OV) has emerged as a promising cancer treatment [3, 4]. It depends on using oncolytic viruses that selectively infect and replicate in tumor cells without harming normal cells [2–5]. Talimogene laherparepvec (T-VEC), an engineered oncolytic virus, has been approved to treat melanoma patients [3]. However, patients with

Received: Apr. 21, 2025.

2020 *Mathematics Subject Classification.* 34D20, 34D23, 37N25, 92B05.

Key words and phrases. cancer; r3LCMV; immunotherapy; CTL; stability.

https://doi.org/10.28924/2291-8639-23-2025-147
ISSN: 2291-8639

impaired immune systems are usually ineligible for this treatment [2]. This highlights the need for more effective cancer therapies.

Lymphocytic choriomeningitis virus (LCMV) is a nonlytic RNA virus [6,7]. It primarily infects rodents and causes either asymptomatic infection or influenza-like illness in humans [6,7]. LCMV has been engineered to produce replication-attenuated viral vectors for cancer immunotherapy [2,7]. These vectors can express tumor antigens that activate cytotoxic T lymphocytes (CTLs) [2,7]. Also, LCMV can evade antibody immune responses [2]. However, there are safety issues regarding the utilization of live LCMV, as it may cause chronic infection [2]. Chronic LCMV infection can make the cancer patient more susceptible to other infections [2]. A recent study has explored an attenuated r3LCMV vector that replicates at lower rates than the wild-type LCMV and does not produce any tumor antigens [2]. Based on this study, injecting tumor-bearing mice with r3LCMV vector enhances tumor control and improves survival [2]. r3LCMV kills tumor cells indirectly through activating virus-specific CTLs that eliminate infected tumor cells, even in the absence of adaptive immune responses [2]. This study has reported the safety and efficacy of r3LCMV vector in mice [2]. However, more studies are needed to examine the safety of this viral vector in greater depth.

Mathematical models have been employed to support clinical studies in testing new promising cancer therapies. For example, Wang et al. [8] developed an oncolytic M1 virotherapy model to determine the minimum dose of M1 needed for tumor elimination. Elaiw et al. [9] extended the model in [8] by considering the diffusion of particles and the effect of CTL immune response. Malinzi et al. [10] proposed a model that examines the combination of OV with chemotherapy. Alzahrani et al. [11] developed a multiscale model that explores the interactions between cancer and oncolytic viruses. Guo and Dobrovolny [12] fitted mathematical models to data from tumors treated by oncolytic adenoviruses. They observed that the data are best fit by a system with immune response [12]. Abernathy et al. [13] used a model to evaluate the sufficient amount of OV required to eradicate tumor cells. Malinzi [14] proposed a model to test the impact of viral spread on tumor cells. Wang et al. [15] studied a virotherapy model with time delays.

In this paper, we continue the work in this field by constructing a within-host r3LCMV cancer immunotherapy model. As mentioned above, an attenuated r3LCMV vector represents a promising cancer treatment, as it has shown safety and efficacy in experimental studies [2]. Therefore, models can help in understanding the interactions between r3LCMV and tumor cells, and the function of immune responses stimulated by this vector. To the best of our knowledge, no r3LCMV immunotherapy model has been formulated yet. The developed model is composed of six ordinary differential equations that explore the relations between nutrient, normal cells, tumor cells, infected tumor cells, viral vector, and virus-specific CTLs. For this model, we

(i) confirm the nonnegativity and boundedness of the solutions, as unbounded or negative solutions are not biologically acceptable,
(ii) compute the equilibrium points along with their existence conditions,

(iii) prove the global stability of equilibria, and
(iv) implement numerical simulations.

2. r3LCMV cancer immunotherapy model

The proposed model takes the form:

$$\begin{cases} \dfrac{dU(t)}{dt} = \mu - \eta_1 UM - \eta_2 UE - \gamma_1 U, \\ \dfrac{dM(t)}{dt} = \alpha_1\eta_1 UM - \gamma_2 M, \\ \dfrac{dE(t)}{dt} = \alpha_2\eta_2 UE - \beta EV - \gamma_3 E, \\ \dfrac{dF(t)}{dt} = \beta EV - \rho FL - \gamma_4 F, \\ \dfrac{dV(t)}{dt} = \dfrac{r}{a}F - \gamma_5 V, \\ \dfrac{dL(t)}{dt} = c\rho FL - \gamma_6 L, \end{cases} \tag{2.1}$$

where $(U, M, E, F, V, L) = (U(t), M(t), E(t), F(t), V(t), L(t))$ express the densities of nutrient, normal cells, tumor cells, infected tumor cells, viral vector, and virus-specific CTLs. Nutrient is produced at rate μ. Normal cells clean out nutrient at rate $\eta_1 UM$ and grow at rate $\alpha_1\eta_1 UM$. Tumor cells clean out nutrient at rate $\eta_2 UE$ and reproduce at rate $\alpha_2\eta_2 UE$. Viral vector infects tumor cells at rate βEV and replicates at rate $\dfrac{r}{a}F$. CTLs are stimulated at rate $c\rho FL$ to kill infected tumor cells at rate ρFL. Nutrient, normal cells, tumor cells, infected tumor cells, viral vector, and virus-specific CTLs decay at rates $\gamma_1 U$, $\gamma_2 M$, $\gamma_3 E$, $\gamma_4 F$, $\gamma_5 V$, and $\gamma_6 L$, respectively. The parameter a stands for the attenuation rate of the viral vector, where $0 < a \leq 1$.

3. Properties of solutions

Theorem 3.1. *The set* $K = \left\{(U, M, E, F, V, L) \in \mathbb{R}^6_+ : 0 \leq U \leq \dfrac{\mu}{\omega}, 0 \leq M \leq \dfrac{\mu\alpha_1}{\omega}, 0 \leq E, F \leq \dfrac{\mu\alpha_2}{\omega}, 0 \leq V \leq \dfrac{r\mu\alpha_2}{a\omega\gamma_5}, 0 \leq L \leq \dfrac{c\mu\alpha_2}{\omega}\right\}$ *is positively invariant set for system* (2.1).

Proof. From system (2.1), we obtain

$$\frac{dU}{dt}|_{U=0} = \mu > 0, \quad \frac{dM}{dt}|_{M=0} = 0, \quad \frac{dE}{dt}|_{E=0} = 0, \quad \frac{dF}{dt}|_{F=0} = \beta EV \geq 0 \; \forall \; E, V \geq 0,$$
$$\frac{dV}{dt}|_{V=0} = \frac{r}{a}F \geq 0 \; \forall \; F \geq 0, \quad \frac{dL}{dt}|_{L=0} = 0.$$

This implies that $(U, M, E, F, V, L) \in \mathbb{R}^6_+$ for $t \geq 0$ whenever $(U(0), M(0), E(0), F(0), V(0), L(0)) \in \mathbb{R}^6_+$.

For boundedness, we pick up the function

$$Z_b = U + \frac{1}{\alpha_1}M + \frac{1}{\alpha_2}E + \frac{1}{\alpha_2}F + \frac{1}{c\alpha_2}L.$$

By evaluating $\frac{dZ_b}{dt}$, we get

$$\begin{aligned}\frac{dZ_b}{dt} =&\mu-\gamma_1 U-\frac{\gamma_2}{\alpha_1}M-\frac{\gamma_3}{\alpha_2}E-\frac{\gamma_4}{\alpha_2}F-\frac{\gamma_6}{c\alpha_2}L\\ \leq&\mu-\omega\left(U+\frac{1}{\alpha_1}M+\frac{1}{\alpha_2}E+\frac{1}{\alpha_2}F+\frac{1}{c\alpha_2}L\right)\\ =&\mu-\omega Z_b,\end{aligned}$$

where $\omega=\min\{\gamma_1,\gamma_2,\gamma_3,\gamma_4,\gamma_5,\gamma_6\}$. This implies that

$$0\leq Z_b\leq\frac{\mu}{\omega}\quad\text{if}\quad Z_b(0)\leq\frac{\mu}{\omega},\ \text{for } t\geq 0.$$

Hence, $U\leq\frac{\mu}{\omega}$, $M\leq\frac{\mu\alpha_1}{\omega}$, $E\leq\frac{\mu\alpha_2}{\omega}$, $F\leq\frac{\mu\alpha_2}{\omega}$, and $L\leq\frac{c\mu\alpha_2}{\omega}$. From the fourth equation of (2.1), we have

$$\begin{aligned}\frac{dV}{dt} =&\frac{r}{a}F-\gamma_5 V\\ \leq&\frac{r\mu\alpha_2}{a\omega}-\gamma_5 V.\end{aligned}$$

This leads to $V\leq\frac{r\mu\alpha_2}{a\omega\gamma_5}$. This proves that K is a positively invariant set. □

Theorem 3.2. *Model* (2.1) *has six equilibrium points:*

(1) The trivial equilibrium Q_0 is always defined;

(2) The normal-cells equilibrium Q_1 exists if $R_0>1$;

(3) The tumor-cells equilibrium Q_2 exists if $R_1>1$;

(4) The infected tumor-cells immune-free equilibrium Q_3 exists if $R_1>1+\frac{a\eta_2\gamma_4\gamma_5}{r\beta\gamma_1}$;

(5) The infected tumor-cells equilibrium Q_4 exists if $R_1>1+\frac{r\beta\gamma_6}{ac\rho\gamma_3\gamma_5}$ and $R_1>1+\frac{r\beta\gamma_6}{ac\rho\gamma_3\gamma_5}+\frac{a\eta_2\gamma_4\gamma_5}{r\beta\gamma_1}+\frac{\eta_2\gamma_4\gamma_6}{c\rho\gamma_1\gamma_3}$;

(6) The infected normal-tumor-cells immune-free equilibrium Q_5 exists if $R_0>1+\frac{a\eta_2\gamma_4\gamma_5}{r\beta\gamma_1}$ and $\frac{\alpha_2\eta_2\gamma_2}{\alpha_1\eta_1\gamma_3}>1$.

Proof. To obtain the equilibria of (2.1), we solve

$$\begin{cases}0=\mu-\eta_1 UM-\eta_2 UE-\gamma_1 U,\\ 0=\alpha_1\eta_1 UM-\gamma_2 M,\\ 0=\alpha_2\eta_2 UE-\beta EV-\gamma_3 E,\\ 0=\beta EV-\rho FL-\gamma_4 F,\\ 0=\frac{r}{a}F-\gamma_5 V,\\ 0=c\rho FL-\gamma_6 L.\end{cases}$$

This gives the following points:

(1) The trivial equilibrium $Q_0=(U_0,0,0,0,0,0)=\left(\frac{\mu}{\gamma_1},0,0,0,0,0\right)$. This point always exists.

(2) The normal-cells equilibrium $Q_1 = (U_1, M_1, 0, 0, 0, 0) = \left(\frac{\gamma_2}{\alpha_1\eta_1}, \frac{\gamma_1}{\eta_1}(R_0 - 1), 0, 0, 0, 0\right)$, where

$$R_0 = \frac{\mu\alpha_1\eta_1}{\gamma_1\gamma_2}.$$

Thus, Q_1 is biologically accepted when $R_0 > 1$. This point simulates the senario of a person who does not have cancer or any signs of disease.

(3) The tumor-cells equilibrium $Q_2 = (U_2, 0, E_2, 0, 0, 0) = \left(\frac{\gamma_3}{\alpha_2\eta_2}, 0, \frac{\gamma_1}{\eta_2}(R_1 - 1), 0, 0, 0\right)$, where

$$R_1 = \frac{\mu\alpha_2\eta_2}{\gamma_1\gamma_3}.$$

Hence, Q_2 is biologically accepted when $R_1 > 1$. This point simulates the scenario of a cancer patient who has not yet received treatment.

(4) The infected tumor-cells immune-free equilibrium

$$\begin{aligned} Q_3 =& (U_3, 0, E_3, F_3, V_3, 0) \\ =& \left(\frac{r\beta\mu}{r\beta\gamma_1 + a\eta_2\gamma_4\gamma_5}, 0, \frac{a\gamma_4\gamma_5}{r\beta}, \frac{a\gamma_1\gamma_3\gamma_5}{r\beta\gamma_1 + a\eta_2\gamma_4\gamma_5}(R_1 - 1 - \frac{a\eta_2\gamma_4\gamma_5}{r\beta\gamma_1}), \frac{r\gamma_1\gamma_3}{r\beta\gamma_1 + a\eta_2\gamma_4\gamma_5}(R_1 - 1 - \frac{a\eta_2\gamma_4\gamma_5}{r\beta\gamma_1}), 0\right). \end{aligned}$$

Thus, Q_3 is biologically accepted if $R_1 > 1 + \frac{a\eta_2\gamma_4\gamma_5}{r\beta\gamma_1}$. This point simulates the situation of a cancer patient who receives r3LCMV cancer immunotherapy, while virus-specific CTLs have not yet been activated.

(5) The infected tumor-cells equilibrium

$$\begin{aligned} Q_4 =& (U_4, 0, E_4, F_4, V_4, L_4) \\ =& \left(\frac{ac\rho\gamma_3\gamma_5 + r\beta\gamma_6}{ac\rho\alpha_2\eta_2\gamma_5}, 0, \frac{ac\rho\gamma_1\gamma_3\gamma_5}{\eta_2(ac\rho\gamma_3\gamma_5 + r\beta\gamma_6)}(R_1 - 1 - \frac{r\beta\gamma_6}{ac\rho\gamma_3\gamma_5}), \frac{\gamma_6}{c\rho}, \frac{r\gamma_6}{ac\rho\gamma_5} \right. \\ & \left., \frac{cr\beta\gamma_1\gamma_3}{\eta_2(ac\rho\gamma_3\gamma_5 + r\beta\gamma_6)}(R_1 - 1 - \frac{r\beta\gamma_6}{ac\rho\gamma_3\gamma_5} - \frac{a\eta_2\gamma_4\gamma_5}{r\beta\gamma_1} - \frac{\eta_2\gamma_4\gamma_6}{c\rho\gamma_1\gamma_3})\right). \end{aligned}$$

Hence, Q_4 is biologically accepted if $R_1 > 1 + \frac{r\beta\gamma_6}{ac\rho\gamma_3\gamma_5}$ and $R_1 > 1 + \frac{r\beta\gamma_6}{ac\rho\gamma_3\gamma_5} + \frac{a\eta_2\gamma_4\gamma_5}{r\beta\gamma_1} + \frac{\eta_2\gamma_4\gamma_6}{c\rho\gamma_1\gamma_3}$. This point simulates the scenario of a cancer patient who receives r3LCMV cancer immunotherapy with active CTLs stimulated by viral vector.

(6) The infected normal-tumor-cells immune-free equilibrium

$$\begin{aligned} Q_5 =& (U_5, M_5, E_5, F_5, V_5, 0) \\ =& \left(\frac{\gamma_2}{\alpha_1\eta_1}, \frac{\gamma_1}{\eta_1}(R_0 - 1 - \frac{a\eta_2\gamma_4\gamma_5}{r\beta\gamma_1}), \frac{a\gamma_4\gamma_5}{r\beta}, \frac{a\gamma_3\gamma_5}{r\beta}(\frac{\alpha_2\eta_2\gamma_2}{\alpha_1\eta_1\gamma_3} - 1), \frac{\gamma_3}{\beta}(\frac{\alpha_2\eta_2\gamma_2}{\alpha_1\eta_1\gamma_3} - 1)\right). \end{aligned}$$

Hence, Q_5 exists when $R_0 > 1 + \frac{a\eta_2\gamma_4\gamma_5}{r\beta\gamma_1}$ and $\frac{\alpha_2\eta_2\gamma_2}{\alpha_1\eta_1\gamma_3} > 1$. This point simulates the scenario of a patient who has normal and tumor cells and receives r3LCMV cancer immunotherapy with inactive immunity.

□

4. Global properties

Let $G_i^{'}$ be the largest invariant subset of $G_i = \left\{(U, M, E, F, V, L) \mid \frac{d\Omega_i}{dt} = 0, i = 0, 1, ..., 5\right\}$.

Theorem 4.1. *The point Q_0 is globally asymptotically stable (GAS) when $R_0 \leq 1$ and $R_1 \leq 1$. It becomes unstable when $R_0 > 1$ or $R_1 > 1$.*

Proof. Take

$$\Omega_0(t) = U_0\left(\frac{U}{U_0} - 1 - \ln\frac{U}{U_0}\right) + \frac{1}{\alpha_1}M + \frac{1}{\alpha_2}E + \frac{1}{\alpha_2}F + \frac{a\gamma_4}{r\alpha_2}V + \frac{1}{c\alpha_2}L.$$

By evaluating the derivative, we get

$$\begin{aligned}
\frac{d\Omega_0}{dt} =& \left(1 - \frac{U_0}{U}\right)(\mu - \eta_1 UM - \eta_2 UE - \gamma_1 U) + \frac{1}{\alpha_1}(\alpha_1\eta_1 UM - \gamma_2 M) + \frac{1}{\alpha_2}(\alpha_2\eta_2 UE - \beta EV - \gamma_3 E) \\
&+ \frac{1}{\alpha_2}(\beta EV - \rho FL - \gamma_4 F) + \frac{a\gamma_4}{r\alpha_2}\left(\frac{r}{a}F - \gamma_5 V\right) + \frac{1}{c\alpha_2}(c\rho FL - \gamma_6 L) \\
=& -\frac{\gamma_1(U - U_0)^2}{U} + \frac{\mu\eta_1}{\gamma_1}M + \frac{\mu\eta_2}{\gamma_1}E - \frac{\gamma_2}{\alpha_1}M - \frac{\gamma_3}{\alpha_2}E - \frac{a\gamma_4\gamma_5}{r\alpha_2}V - \frac{\gamma_6}{c\alpha_2}L \\
=& -\frac{\gamma_1(U - U_0)^2}{U} + \frac{\gamma_2}{\alpha_1}(R_0 - 1)M + \frac{\gamma_3}{\alpha_2}(R_1 - 1)E - \frac{a\gamma_4\gamma_5}{r\alpha_2}V - \frac{\gamma_6}{c\alpha_2}L.
\end{aligned}$$

We observe that $\frac{d\Omega_0}{dt} \leq 0$ when $R_0 \leq 1$ and $R_1 \leq 1$. Additionally, $\frac{d\Omega_0}{dt} = 0$ at $U = U_0$ and $M = E = V = L = 0$. This implies that $\frac{dV}{dt} = 0$. We conclude from the 5^{th} equation of (2.1) that $F = 0$. Hence, $G_0^{'} = \{Q_0\}$ and by LaSalle's invariance principle (LP) [16], Q_0 is GAS if $R_0 \leq 1$ and $R_1 \leq 1$.

To examine the local instability of Q_0 when $R_0 > 1$ or $R_1 > 1$, we use the characteristic equation. The Jacobian matrix at any equilibrium $Q_* = (U_*, M_*, E_*, F_*, V_*, L_*)$ of system (2.1) is given by

$$\mathcal{J}(Q_*) = \begin{bmatrix}
-\eta_1 M_* - \eta_2 E_* - \gamma_1 & -\eta_1 U_* & -\eta_2 U_* & 0 & 0 & 0 \\
\alpha_1\eta_1 M_* & \alpha_1\eta_1 U_* - \gamma_2 & 0 & 0 & 0 & 0 \\
\alpha_2\eta_2 E_* & 0 & \alpha_2\eta_2 U_* - \beta V_* - \gamma_3 & 0 & -\beta E_* & 0 \\
0 & 0 & \beta V_* & -\rho L_* - \gamma_4 & \beta E_* & -\rho F_* \\
0 & 0 & 0 & -\frac{r}{a} & -\gamma_5 & 0 \\
0 & 0 & 0 & c\rho L_* & 0 & c\rho F_* - \gamma_6
\end{bmatrix}.$$

The characteristic equation at Q_0 is computed as

$$(\lambda - \alpha_1\eta_1 U_0 + \gamma_2)(\lambda - \alpha_2\eta_2 U_0 + \gamma_3)(\lambda + \gamma_1)(\lambda + \gamma_4)(\lambda + \gamma_5)(\lambda + \gamma_6) = 0. \tag{4.1}$$

The first two eigenvalues of (4.1) are

$$\begin{aligned}
\lambda_1 =& \alpha_1\eta_1 U_0 - \gamma_2 = \gamma_2\left(\frac{\mu\alpha_1\eta_1}{\gamma_1\gamma_2} - 1\right) = \gamma_2(R_0 - 1) > 0 \text{ if } R_0 > 1, \\
\lambda_2 =& \alpha_2\eta_2 U_0 - \gamma_3 = \gamma_3\left(\frac{\mu\alpha_2\eta_2}{\gamma_1\gamma_3} - 1\right) = \gamma_3(R_1 - 1) > 0 \text{ if } R_1 > 1.
\end{aligned}$$

Thus, Q_0 is unstable when $R_0 > 1$ or $R_1 > 1$. □

Theorem 4.2. *Let $R_0 > 1$. Then, Q_1 is GAS when $\frac{\alpha_2\eta_2\gamma_2}{\alpha_1\eta_1\gamma_3} \leq 1$. It becomes unstable when $\frac{\alpha_2\eta_2\gamma_2}{\alpha_1\eta_1\gamma_3} > 1$.*

Proof. Consider

$$\Omega_1(t) = U_1\left(\frac{U}{U_1} - 1 - \ln\frac{U}{U_1}\right) + \frac{1}{\alpha_1}M_1\left(\frac{M}{M_1} - 1 - \ln\frac{M}{M_1}\right) + \frac{1}{\alpha_2}E + \frac{1}{\alpha_2}F + \frac{a\gamma_4}{r\alpha_2}V + \frac{1}{c\alpha_2}L.$$

The derivative of $\Omega_1(t)$ is given by

$$\begin{aligned}\frac{d\Omega_1}{dt} =& \left(1 - \frac{U_1}{U}\right)(\mu - \eta_1 UM - \eta_2 UE - \gamma_1 U) + \frac{1}{\alpha_1}\left(1 - \frac{M_1}{M}\right)(\alpha_1\eta_1 UM - \gamma_2 M)\\ &+ \frac{1}{\alpha_2}(\alpha_2\eta_2 UE - \beta EV - \gamma_3 E) + \frac{1}{\alpha_2}(\beta EV - \rho FL - \gamma_4 F) + \frac{a\gamma_4}{r\alpha_2}\left(\frac{r}{a}F - \gamma_5 V\right) + \frac{1}{c\alpha_2}(c\rho FL - \gamma_6 L).\end{aligned} \tag{4.2}$$

At equilibrium, Q_1 fulfills

$$\begin{cases}\mu = \eta_1 U_1 M_1 + \gamma_1 U_1,\\ \eta_1 U_1 M_1 = \dfrac{\gamma_2}{\alpha_1} M_1.\end{cases}$$

By applying these conditions and collecting terms, Eq. (4.2) becomes

$$\frac{d\Omega_1}{dt} = -\frac{\gamma_1(U - U_1)^2}{U} + \eta_1 U_1 M_1\left(2 - \frac{U_1}{U} - \frac{U}{U_1}\right) + \frac{\gamma_3}{\alpha_2}\left(\frac{\alpha_2\eta_2\gamma_2}{\alpha_1\eta_1\gamma_3} - 1\right)E - \frac{a\gamma_4\gamma_5}{r\alpha_2}V - \frac{\gamma_6}{c\alpha_2}L.$$

We see that $\frac{d\Omega_1}{dt} \leq 0$ if $\frac{\alpha_2\eta_2\gamma_2}{\alpha_1\eta_1\gamma_3} \leq 1$. Moreover, $\frac{d\Omega_1}{dt} = 0$ when $(U, M, E, F, V, L) = (U_1, M_1, 0, 0, 0, 0)$. Hence, $G_1' = \{Q_1\}$ and Q_1 is GAS when $\frac{\alpha_2\eta_2\gamma_2}{\alpha_1\eta_1\gamma_3} \leq 1$ based on LP [16].

To check the instability of Q_1 when $\frac{\alpha_2\eta_2\gamma_2}{\alpha_1\eta_1\gamma_3} > 1$, we calculate the characteristic equation. The characteristic equation at Q_1 is given by

$$\left[\alpha_1\eta_1^2 U_1 M_1 + (\lambda + \eta_1 M_1 + \gamma_1)(\lambda - \alpha_1\eta_1 U_1 + \gamma_2)\right](\lambda - \alpha_2\eta_2 U_1 + \gamma_3)(\lambda + \gamma_4)(\lambda + \gamma_5)(\lambda + \gamma_6) = 0. \tag{4.3}$$

One of the eignevalues of (4.3) is

$$\lambda = \alpha_2\eta_2 U_1 - \gamma_3 = \gamma_3\left(\frac{\alpha_2\eta_2\gamma_2}{\alpha_1\eta_1\gamma_3} - 1\right) > 0 \text{ if } \frac{\alpha_2\eta_2\gamma_2}{\alpha_1\eta_1\gamma_3} > 1.$$

Hence, Q_1 is unstable if $\frac{\alpha_2\eta_2\gamma_2}{\alpha_1\eta_1\gamma_3} > 1$. □

Theorem 4.3. *Let $R_1 > 1$. Then, Q_2 is GAS when $\frac{\alpha_1\eta_1\gamma_3}{\alpha_2\eta_2\gamma_2} \leq 1$ and $R_1 \leq 1 + \frac{a\eta_2\gamma_4\gamma_5}{r\beta\gamma_1}$.*

Proof. Let

$$\Omega_2(t) = U_2\left(\frac{U}{U_2} - 1 - \ln\frac{U}{U_2}\right) + \frac{1}{\alpha_1}M + \frac{1}{\alpha_2}E_2\left(\frac{E}{E_2} - 1 - \ln\frac{E}{E_2}\right) + \frac{1}{\alpha_2}F + \frac{a\gamma_4}{r\alpha_2}V + \frac{1}{c\alpha_2}L.$$

Then, we get

$$\frac{d\Omega_2}{dt} = \left(1 - \frac{U_2}{U}\right)(\mu - \eta_1 UM - \eta_2 UE - \gamma_1 U) + \frac{1}{\alpha_1}(\alpha_1\eta_1 UM - \gamma_2 M)$$

$$+\frac{1}{\alpha_2}\left(1-\frac{E_2}{E}\right)(\alpha_2\eta_2UE-\beta EV-\gamma_3E)+\frac{1}{\alpha_2}(\beta EV-\rho FL-\gamma_4F)$$
$$+\frac{a\gamma_4}{r\alpha_2}\left(\frac{r}{a}F-\gamma_5V\right)+\frac{1}{c\alpha_2}(c\rho FL-\gamma_6L). \tag{4.4}$$

Q_2 fulfills the following equilibrium conditions

$$\begin{cases}\mu=\eta_2U_2E_2+\gamma_1U_2,\\ \eta_2U_2E_2=\dfrac{\gamma_3}{\alpha_2}E_2.\end{cases}$$

This will convert Eq. (4.4) to

$$\frac{d\Omega_2}{dt}=-\frac{\gamma_1(U-U_2)^2}{U}+\eta_2U_2E_2\left(2-\frac{U_2}{U}-\frac{U}{U_2}\right)+\frac{\gamma_2}{\alpha_1}\left(\frac{\alpha_1\eta_1\gamma_3}{\alpha_2\eta_2\gamma_2}-1\right)M$$
$$+\frac{\beta\gamma_1}{\alpha_2\eta_2}\left(R_1-1-\frac{a\eta_2\gamma_4\gamma_5}{r\beta\gamma_1}\right)V-\frac{\gamma_6}{c\alpha_2}L.$$

We note that $\frac{d\Omega_2}{dt}\leq 0$ if $\frac{\alpha_1\eta_1\gamma_3}{\alpha_2\eta_2\gamma_2}\leq 1$ and $R_1\leq 1+\frac{a\eta_2\gamma_4\gamma_5}{r\beta\gamma_1}$. Also, $\frac{d\Omega_2}{dt}=0$ when $(U,M,E,F,V,L)=(U_2,0,E_2,0,0,0)$. Therefore, $G_2^{'}=\{Q_2\}$ and Q_2 is GAS when $\frac{\alpha_1\eta_1\gamma_3}{\alpha_2\eta_2\gamma_2}\leq 1$ and $R_1\leq 1+\frac{a\eta_2\gamma_4\gamma_5}{r\beta\gamma_1}$ according to LP [16]. □

Theorem 4.4. *Let $R_1>1+\frac{a\eta_2\gamma_4\gamma_5}{r\beta\gamma_1}$. Then, Q_3 is GAS if $R_0\leq 1+\frac{a\eta_2\gamma_4\gamma_5}{r\beta\gamma_1}$ and $R_1\leq 1+\frac{r\beta\gamma_6}{ac\rho\gamma_3\gamma_5}+\frac{a\eta_2\gamma_4\gamma_5}{r\beta\gamma_1}+\frac{\eta_2\gamma_4\gamma_6}{c\rho\gamma_1\gamma_3}$.*

Proof. Consider

$$\Omega_3(t)=U_3\left(\frac{U}{U_3}-1-\ln\frac{U}{U_3}\right)+\frac{1}{\alpha_1}M+\frac{1}{\alpha_2}E_3\left(\frac{E}{E_3}-1-\ln\frac{E}{E_3}\right)+\frac{1}{\alpha_2}F_3\left(\frac{F}{F_3}-1-\ln\frac{F}{F_3}\right)$$
$$+\frac{a\gamma_4}{r\alpha_2}V_3\left(\frac{V}{V_3}-1-\ln\frac{V}{V_3}\right)+\frac{1}{c\alpha_2}L.$$

Then, we obtain

$$\frac{d\Omega_3}{dt}=\left(1-\frac{U_3}{U}\right)(\mu-\eta_1UM-\eta_2UE-\gamma_1U)+\frac{1}{\alpha_1}(\alpha_1\eta_1UM-\gamma_2M)$$
$$+\frac{1}{\alpha_2}\left(1-\frac{E_3}{E}\right)(\alpha_2\eta_2UE-\beta EV-\gamma_3E)+\frac{1}{\alpha_2}\left(1-\frac{F_3}{F}\right)(\beta EV-\rho FL-\gamma_4F)$$
$$+\frac{a\gamma_4}{r\alpha_2}\left(1-\frac{V_3}{V}\right)\left(\frac{r}{a}F-\gamma_5V\right)+\frac{1}{c\alpha_2}(c\rho FL-\gamma_6L). \tag{4.5}$$

At equilibrium, Q_3 satisfies

$$\begin{cases}\mu=\eta_2U_3E_3+\gamma_1U_3,\\ \eta_2U_3E_3=\dfrac{\beta}{\alpha_2}E_3V_3+\dfrac{\gamma_3}{\alpha_2}E_3,\\ \dfrac{\beta}{\alpha_2}E_3V_3=\dfrac{\gamma_4}{\alpha_2}F_3,\\ \dfrac{\gamma_4}{\alpha_2}F_3=\dfrac{a\gamma_4\gamma_5}{r\alpha_2}V_3.\end{cases}$$

By applying these conditions to (4.5), we get

$$\frac{d\Omega_3}{dt} = -\frac{\gamma_1 (U-U_3)^2}{U} + \eta_2 U_3 E_3\left(2 - \frac{U_3}{U} - \frac{U}{U_3}\right) + \frac{r\beta\gamma_1\gamma_2}{\alpha_1(r\beta\gamma_1 + a\eta_2\gamma_4\gamma_5)}\left(R_0 - 1 - \frac{a\eta_2\gamma_4\gamma_5}{r\beta\gamma_1}\right)M + \frac{a\rho\gamma_1\gamma_3\gamma_5}{\alpha_2(r\beta\gamma_1 + a\eta_2\gamma_4\gamma_5)}\left(R_1 - 1 - \frac{r\beta\gamma_6}{ac\rho\gamma_3\gamma_5} - \frac{a\eta_2\gamma_4\gamma_5}{r\beta\gamma_1} - \frac{\eta_2\gamma_4\gamma_6}{c\rho\gamma_1\gamma_3}\right)L.$$

We see that $\frac{d\Omega_3}{dt} \leq 0$ if $R_0 \leq 1 + \frac{a\eta_2\gamma_4\gamma_5}{r\beta\gamma_1}$ and $R_1 \leq 1 + \frac{r\beta\gamma_6}{ac\rho\gamma_3\gamma_5} + \frac{a\eta_2\gamma_4\gamma_5}{r\beta\gamma_1} + \frac{\eta_2\gamma_4\gamma_6}{c\rho\gamma_1\gamma_3}$. Furthermore, $\frac{d\Omega_3}{dt} = 0$ at Q_3. This implies that $G_3^{'} = \{Q_3\}$ and Q_3 is GAS when the above conditions are met based on LP [16].

□

Theorem 4.5. *Let* $R_1 > 1 + \frac{r\beta\gamma_6}{ac\rho\gamma_3\gamma_5}$ *and* $R_1 > 1 + \frac{r\beta\gamma_6}{ac\rho\gamma_3\gamma_5} + \frac{a\eta_2\gamma_4\gamma_5}{r\beta\gamma_1} + \frac{\eta_2\gamma_4\gamma_6}{c\rho\gamma_1\gamma_3}$. *Then,* Q_4 *is GAS when* $1 + \frac{r\beta\gamma_6}{ac\rho\gamma_3\gamma_5} \leq \frac{\alpha_2\eta_2\gamma_2}{\alpha_1\eta_1\gamma_3}$.

Proof. Take

$$\Omega_4(t) = U_4\left(\frac{U}{U_4} - 1 - \ln\frac{U}{U_4}\right) + \frac{1}{\alpha_1}M + \frac{1}{\alpha_2}E_4\left(\frac{E}{E_4} - 1 - \ln\frac{E}{E_4}\right) + \frac{1}{\alpha_2}F_4\left(\frac{F}{F_4} - 1 - \ln\frac{F}{F_4}\right) + \frac{a\gamma_4}{r\alpha_2}V_4\left(\frac{V}{V_4} - 1 - \ln\frac{V}{V_4}\right) + \frac{1}{c\alpha_2}L_4\left(\frac{L}{L_4} - 1 - \ln\frac{L}{L_4}\right).$$

At equilibrium, the following conditions are hold

$$\begin{cases} \mu = \eta_2 U_4 E_4 + \gamma_1 U_4, \\ \eta_2 U_4 E_4 = \frac{\beta}{\alpha_2} E_4 V_4 + \frac{\gamma_3}{\alpha_2} E_4, \\ \frac{\beta}{\alpha_2} E_4 V_4 = \frac{\rho}{\alpha_2} F_4 L_4 + \frac{\gamma_4}{\alpha_2} F_4, \\ \frac{\gamma_4}{\alpha_2} F_4 = \frac{a\gamma_4\gamma_5}{r\alpha_2} V_4, \\ \frac{\rho}{\alpha_2} F_4 L_4 = \frac{\gamma_6}{c\alpha_2} L_4. \end{cases}$$

By applying these conditions and collecting terms, $\frac{d\Omega_4}{dt}$ is given by

$$\frac{d\Omega_4}{dt} = -\frac{\gamma_1 (U-U_4)^2}{U} + \eta_2 U_4 E_4\left(2 - \frac{U_4}{U} - \frac{U}{U_4}\right) + \frac{\rho\eta_1\gamma_3}{\alpha_2\eta_2}\left(1 + \frac{r\beta\gamma_6}{ac\rho\gamma_3\gamma_5} - \frac{\alpha_2\eta_2\gamma_2}{\alpha_1\eta_1\gamma_3}\right)M.$$

Thus, $\frac{d\Omega_4}{dt} \leq 0$ if $1 + \frac{r\beta\gamma_6}{ac\rho\gamma_3\gamma_5} \leq \frac{\alpha_2\eta_2\gamma_2}{\alpha_1\eta_1\gamma_3}$. Additionally, $\frac{d\Omega_4}{dt} = 0$ at Q_4. Hence, $G_4^{'} = \{Q_4\}$ and Q_4 is GAS when $1 + \frac{r\beta\gamma_6}{ac\rho\gamma_3\gamma_5} \leq \frac{\alpha_2\eta_2\gamma_2}{\alpha_1\eta_1\gamma_3}$ based on LP [16]. □

Theorem 4.6. *Assume that* $R_0 > 1 + \frac{a\eta_2\gamma_4\gamma_5}{r\beta\gamma_1}$ *and* $\frac{\alpha_2\eta_2\gamma_2}{\alpha_1\eta_1\gamma_3} > 1$. *Then,* Q_5 *is GAS when* $\frac{\alpha_2\eta_2\gamma_2}{\alpha_1\eta_1\gamma_3} \leq 1 + \frac{r\beta\gamma_6}{ac\rho\gamma_3\gamma_5}$.

Proof. Take

$$\Omega_5(t) = U_5\left(\frac{U}{U_5} - 1 - \ln\frac{U}{U_5}\right) + \frac{1}{\alpha_1}M_5\left(\frac{M}{M_5} - 1 - \ln\frac{M}{M_5}\right) + \frac{1}{\alpha_2}E_5\left(\frac{E}{E_5} - 1 - \ln\frac{E}{E_5}\right) + \frac{1}{\alpha_2}F_5\left(\frac{F}{F_5} - 1 - \ln\frac{F}{F_5}\right) + \frac{a\gamma_4}{r\alpha_2}V_5\left(\frac{V}{V_5} - 1 - \ln\frac{V}{V_5}\right) + \frac{1}{c\alpha_2}L.$$

At equilibrium, Q_5 satisfies

$$\begin{cases} \mu = \eta_1 U_5 M_5 + \eta_2 U_5 E_5 + \gamma_1 U_5, \\ \eta_1 U_5 M_5 = \dfrac{\gamma_2}{\alpha_2} M_5, \\ \eta_2 U_5 E_5 = \dfrac{\beta}{\alpha_2} E_5 V_5 + \dfrac{\gamma_3}{\alpha_2} E_5, \\ \dfrac{\beta}{\alpha_2} E_5 V_5 = \dfrac{\gamma_4}{\alpha_2} F_5, \\ \dfrac{\gamma_4}{\alpha_2} F_5 = \dfrac{a\gamma_4\gamma_5}{r\alpha_2} V_5. \end{cases}$$

By applying these conditions, we get

$$\frac{d\Omega_5}{dt} = -\frac{\gamma_1 (U - U_5)^2}{U} + \eta_2 U_5 M_5\left(2 - \frac{U_5}{U} - \frac{U}{U_5}\right) + \eta_2 U_5 E_5\left(2 - \frac{U_5}{U} - \frac{U}{U_5}\right) + \frac{\rho a\gamma_3\gamma_5}{r\beta\alpha_2}\left(\frac{\alpha_2\eta_2\gamma_2}{\alpha_1\eta_1\gamma_3} - 1 - \frac{r\beta\gamma_6}{ac\rho\gamma_3\gamma_5}\right)L.$$

Thus, $\frac{d\Omega_5}{dt} \leq 0$ if $\frac{\alpha_2\eta_2\gamma_2}{\alpha_1\eta_1\gamma_3} \leq 1 + \frac{r\beta\gamma_6}{ac\rho\gamma_3\gamma_5}$. Additionally, $\frac{d\Omega_5}{dt} = 0$ at Q_5. Hence, $G_5^{'} = \{Q_5\}$ and Q_5 is GAS when $\frac{\alpha_2\eta_2\gamma_2}{\alpha_1\eta_1\gamma_3} \leq 1 + \frac{r\beta\gamma_6}{ac\rho\gamma_3\gamma_5}$ based on LP [16]. □

5. Numerical simulations

This section simulates the results obtained in the previous sections. The MATLAB solver ode45 is used to execute the simulations. To ensure the global stability with any initial conditions, we randomly choose three sets of initial values:

I-1 : $(U(0), M(0), E(0), F(0), V(0), L(0)) = (0.1, 0.2, 0.1, 0.01, 0.03, 0.1)$.

I-2 : $(U(0), M(0), E(0), F(0), V(0), L(0)) = (0.3, 0.1, 0.03, 0.02, 0.01, 0.2)$.

I-3 : $(U(0), M(0), E(0), F(0), V(0), L(0)) = (0.2, 0.3, 0.05, 0.03, 0.04, 0.07)$.

The results are partitioned into six cases that correspond to the stability of each equilibrium point. We consider $a = 1$ and vary β, ρ, η_1, η_2, γ_5, and γ_6. The remaining parameters are fixed to the values presented in Table 1. The cases are:

(1) We opt $\beta = 0.55$, $\rho = 0.5$, $\eta_1 = 0.03$, $\eta_2 = 0.03$, $\gamma_5 = 0.5$, and $\gamma_6 = 0.1$. This gives $R_0 = 0.8 < 1$ and $R_1 = 0.4 < 1$. Hence, $Q_0 = (1, 0, 0, 0, 0, 0)$ is GAS as proved in Theorem 4.1 (Figure 1).

(2) We opt $\beta = 0.55$, $\rho = 0.5$, $\eta_1 = 0.05$, $\eta_2 = 0.03$, $\gamma_5 = 0.5$, and $\gamma_6 = 0.1$. The thresholds are $R_0 = 1.33 > 1$ and $\frac{\alpha_2\eta_2\gamma_2}{\alpha_1\eta_1\gamma_3} = 0.3 < 1$. Thus, $Q_1 = (0.75, 0.13, 0, 0, 0, 0)$ is GAS as proved in Theorem 4.2 (Figure 2). The person either does not have cancer or has been healed from it.

(3) We opt $\beta = 0.55$, $\rho = 0.5$, $\eta_1 = 0.03$, $\eta_2 = 0.09$, $\gamma_5 = 0.5$, and $\gamma_6 = 0.1$. This gives $R_1 = 1.2 > 1$, $\frac{\alpha_1\eta_1\gamma_3}{\alpha_2\eta_2\gamma_2} = 0.6667 < 1$, and $R_1 < 2.0227 = 1 + \frac{a\eta_2\gamma_4\gamma_5}{r\beta\gamma_1}$. Therefore, $Q_2 = (0.83, 0, 0.04, 0, 0, 0)$ is GAS as indicated in Theorem 4.3 (Figure 3). In this case, the cancer patient has not yet received treatment.

(4) We opt $\beta = 0.99$, $\rho = 0.5$, $\eta_1 = 0.03$, $\eta_2 = 0.09$, $\gamma_5 = 0.09$, and $\gamma_6 = 0.1$. The thresholds are $R_1 = 1.2 > 1.1023 = 1 + \frac{a\eta_2\gamma_4\gamma_5}{r\beta\gamma_1}$, $R_0 = 0.8 < 1.1023 = 1 + \frac{a\eta_2\gamma_4\gamma_5}{r\beta\gamma_1}$, and $R_1 < 98.1023 = 1 + \frac{r\beta\gamma_6}{ac\rho\gamma_3\gamma_5} + \frac{a\eta_2\gamma_4\gamma_5}{r\beta\gamma_1} + \frac{\eta_2\gamma_4\gamma_6}{c\rho\gamma_1\gamma_3}$. Hence, $Q_3 = (0.91, 0, 0.0227, 0.002, 0.005, 0)$ is GAS as indicated in Theorem 4.4 (Figure 4). Here, the cancer patient receives r3LCMV cancer therapy. However, CTLs have not yet been activated.

(5) We opt $\beta = 0.9$, $\rho = 2.9$, $\eta_1 = 0.01$, $\eta_2 = 0.2$, $\gamma_5 = 0.09$, and $\gamma_6 = 0.003$. This gives $R_1 = 2.6667 > 1.4138 = 1 + \frac{r\beta\gamma_6}{ac\rho\gamma_3\gamma_5}$, $R_1 > 1.7672 = 1 + \frac{r\beta\gamma_6}{ac\rho\gamma_3\gamma_5} + \frac{a\eta_2\gamma_4\gamma_5}{r\beta\gamma_1} + \frac{\eta_2\gamma_4\gamma_6}{c\rho\gamma_1\gamma_3}$, and $1 + \frac{r\beta\gamma_6}{ac\rho\gamma_3\gamma_5} < 10 = \frac{\alpha_2\eta_2\gamma_2}{\alpha_1\eta_1\gamma_3}$. Thus, $Q_4 = (0.53, 0, 0.089, 0.01, 0.028, 0.05)$ is GAS as proved in Theorem 4.5 (Figure 5). The cancer patient here receives r3LCMV therapy with active CTLs.

(6) We opt $\beta = 0.9$, $\rho = 2.9$, $\eta_1 = 0.08$, $\eta_2 = 0.2$, $\gamma_5 = 0.09$, and $\gamma_6 = 0.1$. The thresholds are $R_0 = 2.1333 > 1.25 = 1 + \frac{a\eta_2\gamma_4\gamma_5}{r\beta\gamma_1}$, $\frac{\alpha_2\eta_2\gamma_2}{\alpha_1\eta_1\gamma_3} = 1.25 > 1$, and $\frac{\alpha_2\eta_2\gamma_2}{\alpha_1\eta_1\gamma_3} < 14.7931 = 1 + \frac{r\beta\gamma_6}{ac\rho\gamma_3\gamma_5}$. Thus, $Q_5 = (0.47, 0.22, 0.025, 0.006, 0.017, 0)$ is GAS as proved in Theorem 4.6 (Figure 6). Here, the patient has normal and tumor cells, and he receives r3LCMV therapy with inactive CTLs.

Effect of the parameters a and c on tumor cells. To note the effect of changing the value of the attenuation rate (a) on tumor cells, we consider the same values used in case (5) and vary only the value of a. Figure 7 shows that large values of a increase the concentration of tumor cells. Thus, the attenuation rate of viral vector can have a large impact on its role in eliminating tumor cells from the body.

To observe the impact of changing the stimulation rate of virus-specific CTLs (c) on tumor cells, we consider the same values used in case (5) and vary only the value of c. Figure 8 shows that increasing the value of c decreases the concentration of infected tumor cells. Hence, the stimulation rate of virus-specific CTLs induced by viral vector plays a key role in eliminating tumor cells from the body.

6. Discussion and future works

An attenuated r3LCMV vector has demonstrated safety and efficacy in treating cancer [2]. Mathematical models have supported experimental studies in testing and investigating new promising cancer therapies. In this work, we construct a within-host r3LCMV cancer immunotherapy model.

The model is composed of six equations that describe the interactions between nutrient, normal cells, tumor cells, infected tumor cells, viral vector, and virus-specific CTLs. It has six equilibria as the following:

(1) The trivial equilibrium Q_0 is defined and GAS when $R_0 \leq 1$ and $R_1 \leq 1$.
(2) The normal-cells equilibrium Q_1 is defined and GAS when $R_0 > 1$ and $\frac{\alpha_2\eta_2\gamma_2}{\alpha_1\eta_1\gamma_3} \leq 1$.
(3) The tumor-cells equilibrium Q_2 is defined and GAS when $R_1 > 1$, $\frac{\alpha_1\eta_1\gamma_3}{\alpha_2\eta_2\gamma_2} \leq 1$, and $R_1 \leq 1 + \frac{a\eta_2\gamma_4\gamma_5}{r\beta\gamma_1}$.
(4) The infected tumor-cells immune-free equilibrium Q_3 is defined and GAS when $R_1 > 1 + \frac{a\eta_2\gamma_4\gamma_5}{r\beta\gamma_1}$, $R_0 \leq 1 + \frac{a\eta_2\gamma_4\gamma_5}{r\beta\gamma_1}$, and $R_1 \leq 1 + \frac{r\beta\gamma_6}{ac\rho\gamma_3\gamma_5} + \frac{a\eta_2\gamma_4\gamma_5}{r\beta\gamma_1} + \frac{\eta_2\gamma_4\gamma_6}{c\rho\gamma_1\gamma_3}$.
(5) The infected tumor-cells equilibrium Q_4 is defined and GAS when $R_1 > 1 + \frac{r\beta\gamma_6}{ac\rho\gamma_3\gamma_5}$, $R_1 > 1 + \frac{r\beta\gamma_6}{ac\rho\gamma_3\gamma_5} + \frac{a\eta_2\gamma_4\gamma_5}{r\beta\gamma_1} + \frac{\eta_2\gamma_4\gamma_6}{c\rho\gamma_1\gamma_3}$, and $1 + \frac{r\beta\gamma_6}{ac\rho\gamma_3\gamma_5} \leq \frac{\alpha_2\eta_2\gamma_2}{\alpha_1\eta_1\gamma_3}$.
(6) The infected normal-tumor-cells immune-free equilibrium Q_5 is defined and GAS when $R_0 > 1 + \frac{a\eta_2\gamma_4\gamma_5}{r\beta\gamma_1}$, $\frac{\alpha_2\eta_2\gamma_2}{\alpha_1\eta_1\gamma_3} > 1$, and $\frac{\alpha_2\eta_2\gamma_2}{\alpha_1\eta_1\gamma_3} \leq 1 + \frac{r\beta\gamma_6}{ac\rho\gamma_3\gamma_5}$.

We found a perfect match between theorems and numerical simulations. The equilibria of model (2.1) simulate four main states: a healthy individual without cancer, a cancer patient who does not receive any treatments, a cancer patient who receives r3LCMV cancer therapy with inactive immunity, and a cancer patient who receives r3LCMV therapy with active virus-specific CTLs. The conversions between these states depend on the model's parameters. In addition, we observe that increasing the stimulation rate of CTLs induced by r3LCMV viral vector reduces the concentration of infected tumor cells. Thus, the stimulation of CTLs can eliminate the tumor. Furthermore, we note that the attenuation rate of the viral vector affects its ability to eliminate tumor cells from the body. Therefore, the values of these parameters need to be carefully picked. The model can support experimental studies in understanding the role of r3LCMV in eliminating tumor cells. Also, it can help in identifying the most effective attenuation and stimulation rates of viral vector and CTLs, respectively. The principal limitation of the current work is the lack of real data for simulations. We took values from previous studies as no real data are available. When real data become available, fitting the model with real data can give a deeper insight into the role of r3LCMV in treating cancer. Model (2.1) can be developed by:

(i) Fitting with real data to get a better estimation of model's parameters;
(ii) Taking into consideration the diffusion of viral vectors, which will convert the equations into partial differential equations;
(iii) Considering the time delay that may happen within some biological processes;
(iv) Comparing the model results with real data.

TABLE 1. Parameters' values of model (2.1).

Parameter	Value	Reference
μ	0.02	[8]
η_1	Varied	–
η_2	Varied	–
α_1	0.8	[8]
α_2	0.8	[8]
β	Varied	–
ρ	Varied	–
r	0.24	[17]
a	$0 < a \leq 1$	–
c	0.1	[18]
γ_1	0.02	[8]
γ_2	0.03	[8]
γ_3	0.06	[8]
γ_4	0.06	[8]
γ_5	Varied	–
γ_6	Varied	–

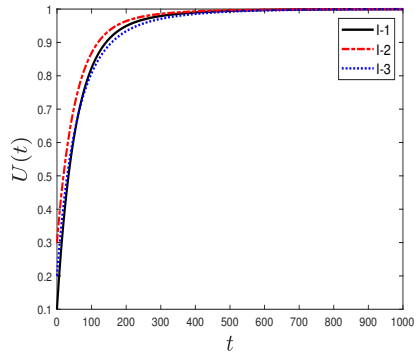

(A) Nutrient

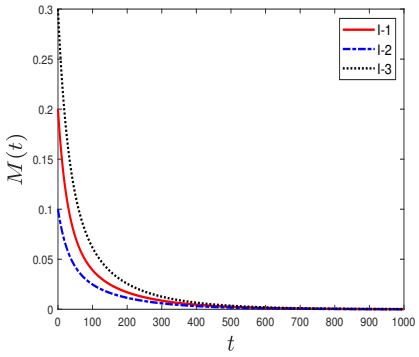

(B) Normal cells

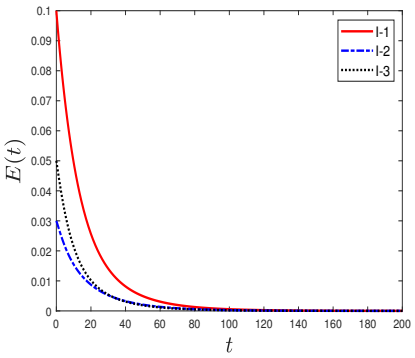

(C) Tumor cells

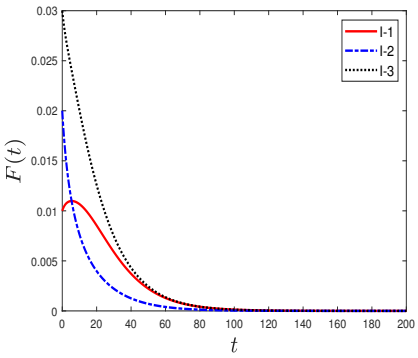

(D) Infected tumor cells

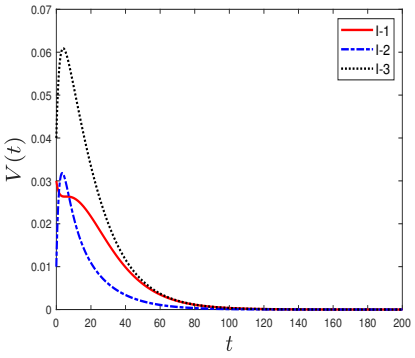

(E) Viral vector

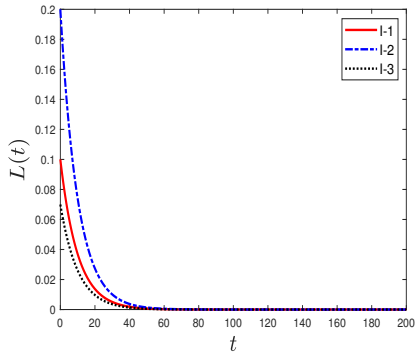

(F) Virus-specific CTLs

FIGURE 1. The numerical results of model (2.1) for $\beta = 0.55$, $\rho = 0.5$, $\eta_1 = 0.03$, $\eta_2 = 0.03$, $\gamma_5 = 0.5$, and $\gamma_6 = 0.1$ The point $Q_0 = (1, 0, 0, 0, 0, 0)$ is GAS.

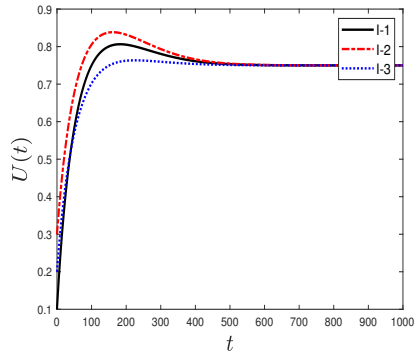

(A) Nutrient

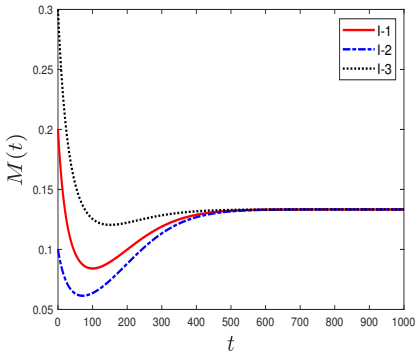

(B) Normal cells

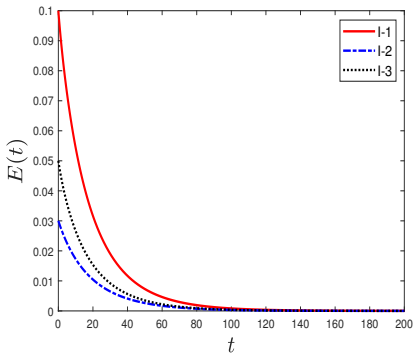

(C) Tumor cells

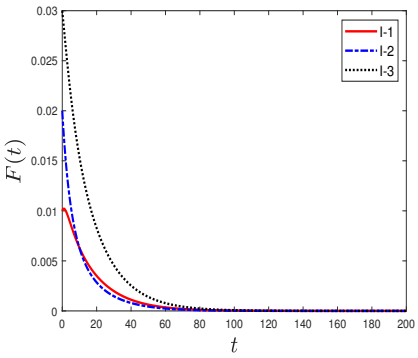

(D) Infected tumor cells

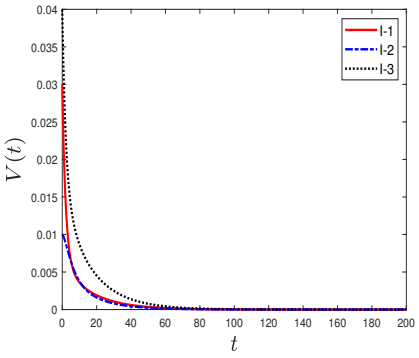

(E) Viral vector

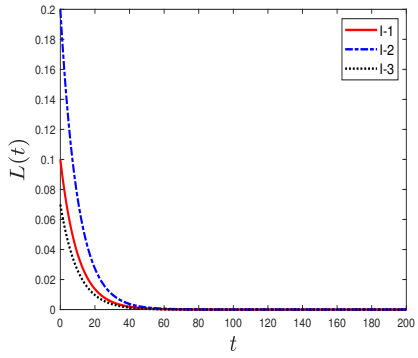

(F) Virus-specific CTLs

FIGURE 2. The numerical results of model (2.1) for $\beta = 0.55$, $\rho = 0.5$, $\eta_1 = 0.05$, $\eta_2 = 0.03$, $\gamma_5 = 0.5$, and $\gamma_6 = 0.1$. The point $Q_1 = (0.75, 0.13, 0, 0, 0, 0)$ is GAS.

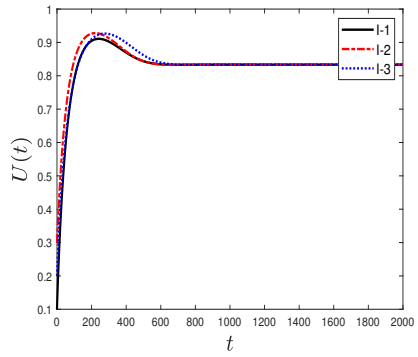

(A) Nutrient

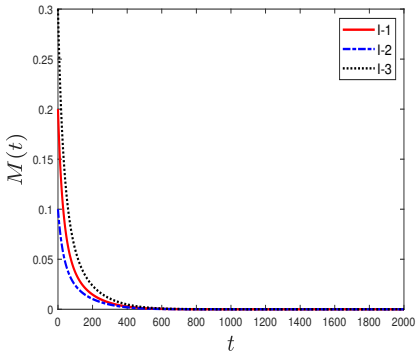

(B) Normal cells

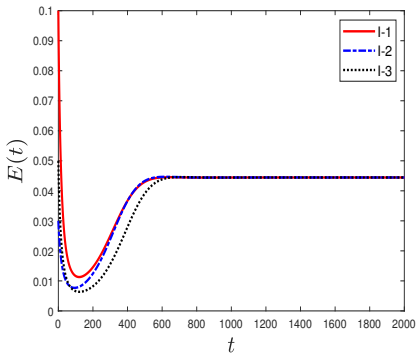

(C) Tumor cells

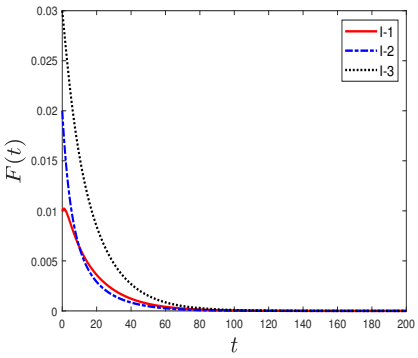

(D) Infected tumor cells

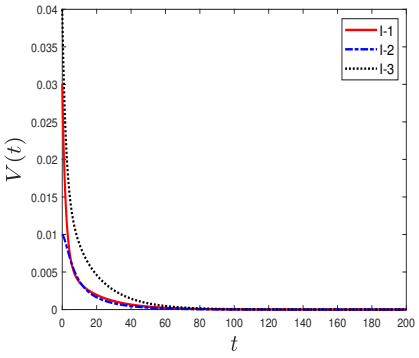

(E) Viral vector

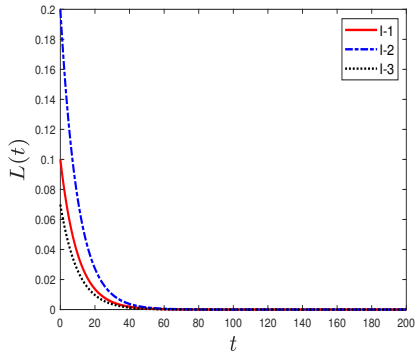

(F) Virus-specific CTLs

FIGURE 3. The numerical results of model (2.1) for $\beta = 0.55$, $\rho = 0.5$, $\eta_1 = 0.03$, $\eta_2 = 0.09$, $\gamma_5 = 0.5$, and $\gamma_6 = 0.1$. The point $Q_2 = (0.83, 0, 0.04, 0, 0, 0)$ is GAS.

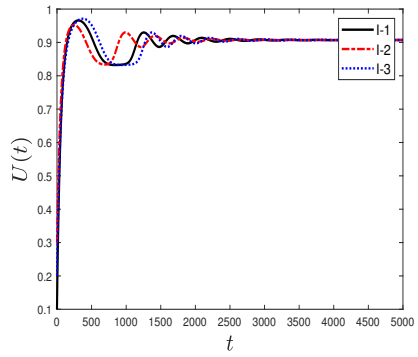

(A) Nutrient

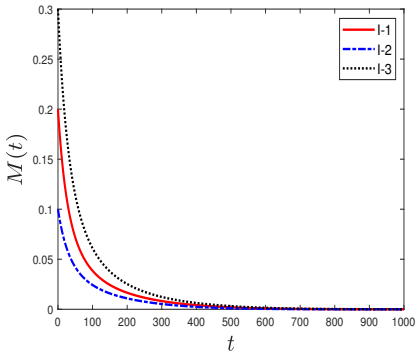

(B) Normal cells

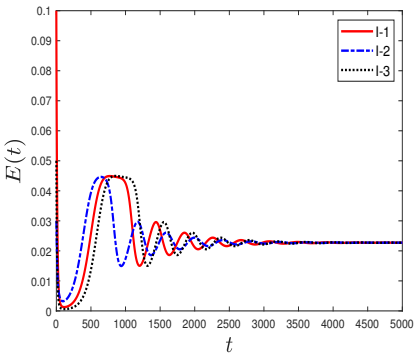

(C) Tumor cells

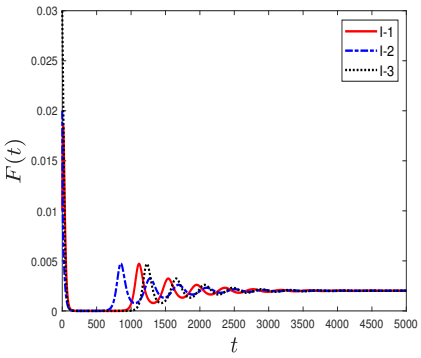

(D) Infected tumor cells

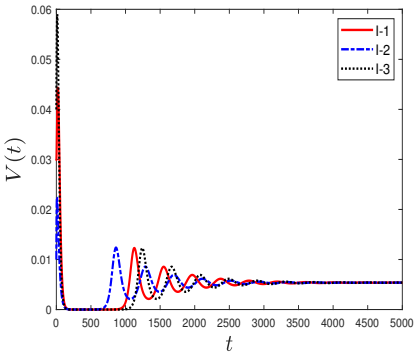

(E) Viral vector

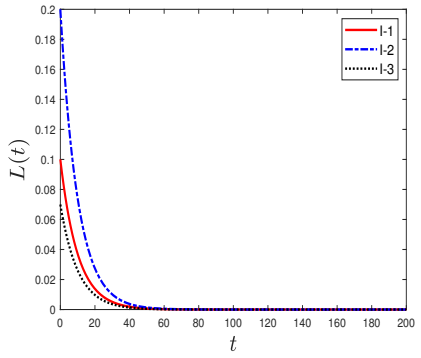

(F) Virus-specific CTLs

FIGURE 4. The numerical results of model (2.1) for $\beta = 0.99$, $\rho = 0.5$, $\eta_1 = 0.03$, $\eta_2 = 0.09$, $\gamma_5 = 0.09$, and $\gamma_6 = 0.1$. The point $Q_3 = (0.91, 0, 0.0227, 0.002, 0.005, 0)$ is GAS.

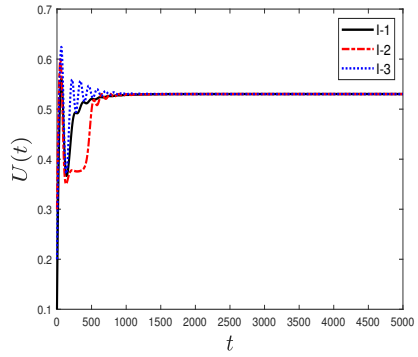

(A) Nutrient

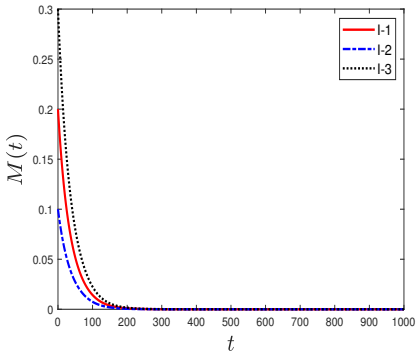

(B) Normal cells

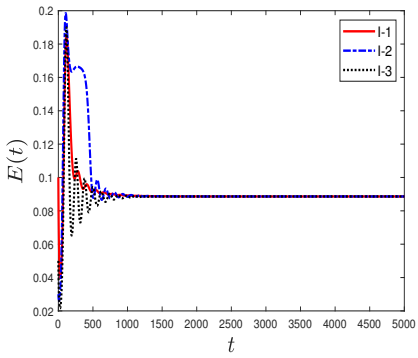

(C) Tumor cells

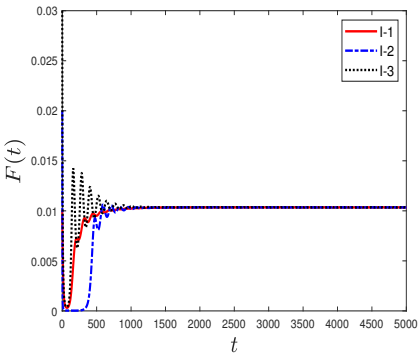

(D) Infected tumor cells

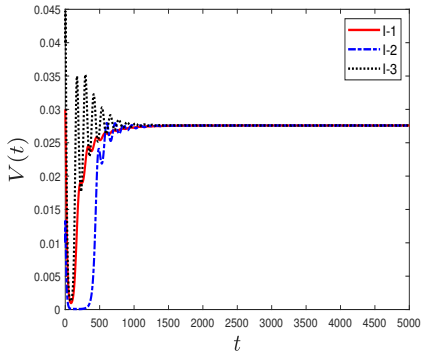

(E) Viral vector

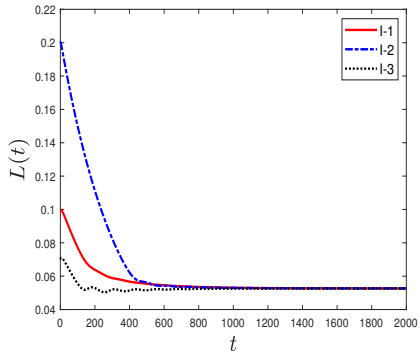

(F) Virus-specific CTLs

FIGURE 5. The numerical results of model (2.1) for $\beta = 0.9$, $\rho = 2.9$, $\eta_1 = 0.01$, $\eta_2 = 0.2$, $\gamma_5 = 0.09$, and $\gamma_6 = 0.003$. The point $Q_4 = (0.53, 0, 0.089, 0.01, 0.028, 0.05)$ is GAS.

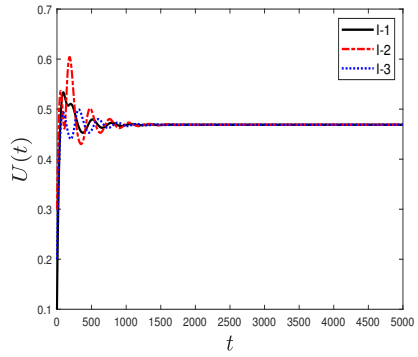

(A) Nutrient

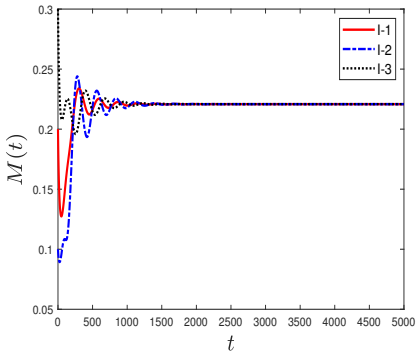

(B) Normal cells

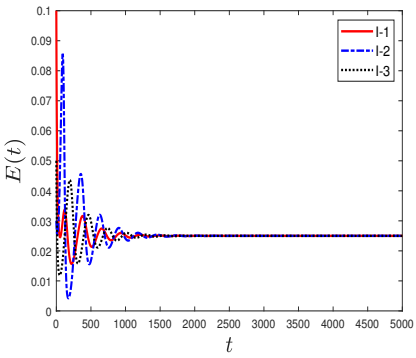

(C) Tumor cells

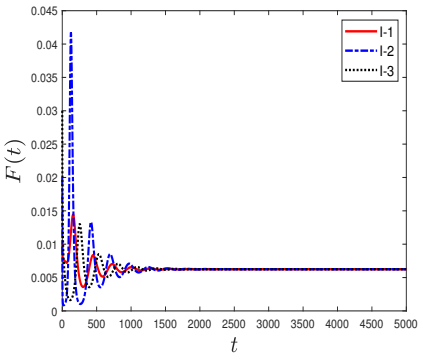

(D) Infected tumor cells

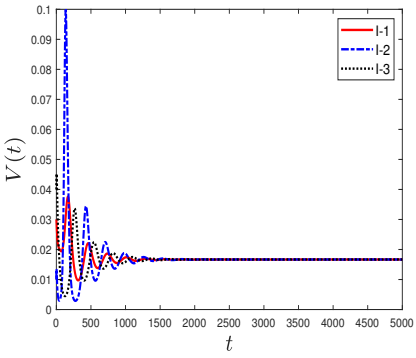

(E) Viral vector

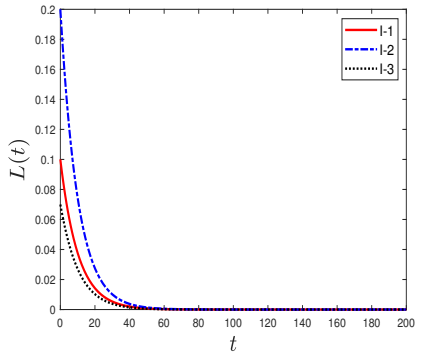

(F) Virus-specific CTLs

FIGURE 6. The numerical results of model (2.1) for $\beta = 0.9$, $\rho = 2.9$, $\eta_1 = 0.08$, $\eta_2 = 0.2$, $\gamma_5 = 0.09$, and $\gamma_6 = 0.1$. The point $Q_5 = (0.47, 0.22, 0.025, 0.006, 0.017, 0)$ is GAS.

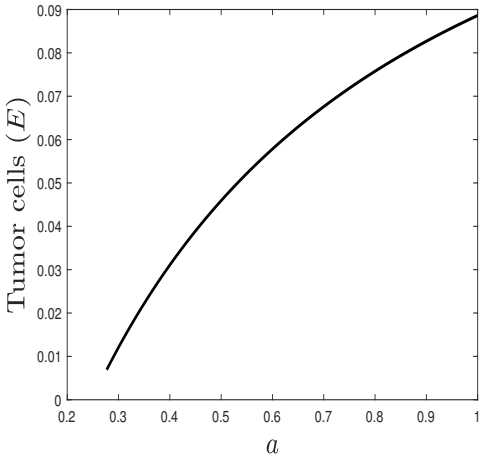

FIGURE 7. The impact of varying the attenuation rate of viral vector (a) on the concentration of tumor cells. The parameters are $\beta = 0.9$, $\rho = 2.9$, $\eta_1 = 0.01$, $\eta_2 = 0.2$, $\gamma_5 = 0.09$, and $\gamma_6 = 0.003$.

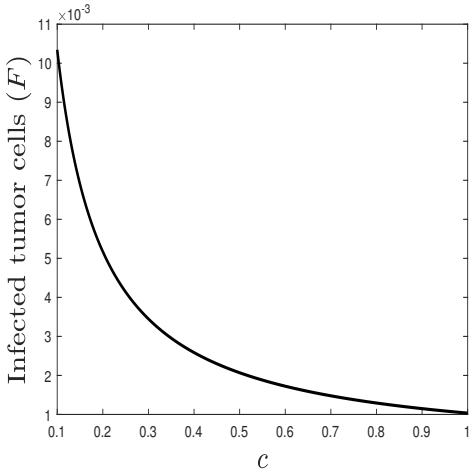

FIGURE 8. The impact of varying the stimulation rate of virus-specific CTLs (c) on the concentration of infected tumor cells. The parameters are $\beta = 0.9$, $\rho = 2.9$, $\eta_1 = 0.01$, $\eta_2 = 0.2$, $\gamma_5 = 0.09$, and $\gamma_6 = 0.003$.

Acknowledgments: The authors acknowledge that this project was funded by the Deanship of Scientific Research (DSR), University of Business and Technology, Jeddah 21361, Saudi Arabia. The authors, therefore, gratefully acknowledge the DSR technical and financial support.

Conflicts of Interest: The author declares that there are no conflicts of interest regarding the publication of this paper.

References

[1] American Cancer Society, American Cancer Society Releases Latest Global Cancer Statistics; Cancer Cases Expected to Rise to 35 Million Worldwide by 2050, The ASCO Post, 2024.

[2] Y.R. Chung, B. Awakoaiye, T. Dangi, N. Irani, S. Fourati, P. Penaloza-MacMaster, An Attenuated Lymphocytic Choriomeningitis Virus Vector Enhances Tumor Control in Mice Partly Via IFN-I, J. Clin. Invest. 134 (2024), e178945. https://doi.org/10.1172/jci178945.

[3] A.D. Al Agha, Analysis of a Reaction-diffusion Oncolytic Sars-cov-2 Model, Model. Earth Syst. Environ. 10 (2024), 4641–4662. https://doi.org/10.1007/s40808-024-02009-z.

[4] A.A. Agha, H.A. Garalleh, Oncolysis by Sars-cov-2: Modeling and Analysis, AIMS Math. 9 (2024), 7212–7252. https://doi.org/10.3934/math.2024351.

[5] A. Friedman, X. Lai, Combination Therapy for Cancer with Oncolytic Virus and Checkpoint Inhibitor: A Mathematical Model, PLOS ONE 13 (2018), e0192449. https://doi.org/10.1371/journal.pone.0192449.

[6] M. Purde, J. Cupovic, Y.A. Palmowski, et al. A Replicating Lcmv-based Vaccine for the Treatment of Solid Tumors, Mol. Therapy 32 (2024), 426–439. https://doi.org/10.1016/j.ymthe.2023.11.026.

[7] C. Gomar, C.A. Di Trani, A. Bella, et al. Efficacy of Lcmv-based Cancer Immunotherapies Is Unleashed by Intratumoral Injections of Polyi:c, J. ImmunoTher. Cancer 12 (2024), e008287. https://doi.org/10.1136/jitc-2023-008287.

[8] Z. Wang, Z. Guo, H. Peng, A Mathematical Model Verifying Potent Oncolytic Efficacy of M1 Virus, Math. Biosci. 276 (2016), 19-27. https://doi.org/10.1016/j.mbs.2016.03.001.

[9] A. Elaiw, A. Hobiny, A. Al Agha, Global Dynamics of Reaction-diffusion Oncolytic M1 Virotherapy with Immune Response, Appl. Math. Comput. 367 (2020), 124758. https://doi.org/10.1016/j.amc.2019.124758.

[10] J. Malinzi, R. Ouifki, A. Eladdadi, et al. Enhancement of Chemotherapy Using Oncolytic Virotherapy: Mathematical and Optimal Control Analysis, Math. Biosci. Eng. 15 (2018), 1435–1463. https://doi.org/10.3934/mbe.2018066.

[11] T. Alzahrani, R. Eftimie, D. Trucu, Multiscale Modelling of Cancer Response to Oncolytic Viral Therapy, Math. Biosci. 310 (2019), 76-95. https://doi.org/10.1016/j.mbs.2018.12.018.

[12] E. Guo, H.M. Dobrovolny, Mathematical Modeling of Oncolytic Virus Therapy Reveals Role of the Immune Response, Viruses 15 (2023), 1812. https://doi.org/10.3390/v15091812.

[13] Z. Abernathy, K. Abernathy, J. Stevens, et al. A Mathematical Model for Tumor Growth and Treatment Using Virotherapy, AIMS Math. 5 (2020), 4136–4150. https://doi.org/10.3934/math.2020265.

[14] J. Malinzi, A Mathematical Model for Oncolytic Virus Spread Using the Telegraph Equation, Commun. Nonlinear Sci. Numer. Simul. 102 (2021), 105944. https://doi.org/10.1016/j.cnsns.2021.105944.

[15] S. Wang, S. Wang, X. Song, Hopf Bifurcation Analysis in a Delayed Oncolytic Virus Dynamics with Continuous Control, Nonlinear Dyn. 67 (2011), 629-640. https://doi.org/10.1007/s11071-011-0015-5.

[16] H.K. Khalil, Nonlinear Systems, Prentice-Hall, (1996).

[17] C. Li, J. Xu, J. Liu, et al. The Within-Host Viral Kinetics of SARS-CoV-2, Math. Biosci. Eng. 17 (2020), 2853–2861. https://doi.org/10.3934/mbe.2020159.

[18] A. KOROBEINIKOV, Global Properties of Basic Virus Dynamics Models, Bull. Math. Biol. 66 (2004), 879-883. https://doi.org/10.1016/j.bulm.2004.02.001.